Plasma Sci. Technol. **26** (2024) 075505 (8pp) https://doi.org/10.1088/2058-6272/ad3499

Fast synthesis of gold nanoparticles by cold atmospheric pressure plasma jet in the presence of Au^+ ions and a capping agent

Tatiana HABIB[1,2,*], **José Mauricio A. CAIUT**[2] **and Bruno CAILLIER**[1]

[1] Laboratoire Diagnostics des Plasmas Hors Equilibre (DPHE), Université de Toulouse, INU Champollion, Albi 81000, France
[2] Department of Chemistry, The Nanomaterials and Luminescent Systems Group, Faculty of Philosophy, Science and Letters at Ribeirão Preto, University of São Paulo, Ribeirão Preto-SP 14040-901, Brazil

[*]E-mail of corresponding author: tatiana.habib@univ-tlse3.fr

Received 11 December 2023, revised 13 March 2024
Accepted for publication 15 March 2024
Published 24 May 2024

Abstract

Homogeneous gold nanoparticles were synthesized under atmospheric pressure using a non-thermal helium plasma jet in a single-step process. A current power supply was used to generate the plasma discharge rich in diverse reactive species. These species induce rapid chemical reactions responsible for the reduction of the gold salts upon contact with the liquid solution. In this study, spherical and monodispersed gold nanoparticles were obtained within 5 min of plasma exposure using a solution containing gold (III) chloride hydrate ($HAuCl_4$) as a precursor and polyvinylpyrrolidone (PVP) as a capping agent to inhibit agglomerations. The formation of these metal nanoparticles was initially perceptible through a visible change in the sample's color, transitioning from light yellow to a red/pink color. This was subsequently corroborated by UV-vis spectroscopy, which revealed an optical absorption in the 520–550 nm range for Au NPs, corresponding to the surface plasmon resonance (SPR) band. An investigation into the impact of various parameters, including plasma discharge duration, precursor and capping agent concentrations, was carried out to optimize conditions for the formation of well-separated, spherical gold nanoparticles. Dynamic light scattering (DLS) was used to measure the size of these nanoparticles, transmission electron microscopy (TEM) was used to observe their morphology and X-ray diffraction (XRD) was also employed to determine their crystallographic structure. The results confirm that homogeneous spherical gold nanoparticles with an average diameter of 13 nm can be easily synthesized through a rapid, straightforward, and environmentally friendly approach utilizing a helium atmospheric pressure plasma.

Supplementary material for this article is available online

Keywords: gold nanoparticles, non-thermal, plasma jet, helium, DBD

(Some figures may appear in colour only in the online journal)

1. Introduction

In today's biotechnological sciences and industry, nanotechnology plays a significant and gradually growing role [1]. It is a technique that can achieve high levels of precision in size, material shapes, components and functions by the manipulation of matter on a near-atomic scale [2]. Nanomaterials can be defined as materials with at least one dimension less than 100 nanometers and they come in a variety of shapes including nanofibers, nanolayers, nanoparticles, etc [3]. Nanoparticles have a wide range of size-dependent properties (mechanical, optical, electrical, and magnetic) that are

[*] Author to whom any correspondence should be addressed.

very different or not found in their bulk materials [4, 5]. They have high reactivity due to their high surface area-to-volume ratio which can result in the formation of agglomerations and bigger particles [1]. Depending on the size of the agglomerate, nanoparticles can behave like larger particles. So, a precise control over the shape and size of these nanoparticles is needed and their surface reactivity must be considered when evaluating new materials [6]. Metal nanoparticles in particular have attracted increasing interest due to their versatile applications that can improve the quality of life in the near future such as nanomedicine, biomedical sensing devices, electric devices, gas sensors, catalysis, etc [6–9]. Among the various metals, gold nanoparticles are currently the main subject of recent studies because they possess distinctive properties such as optical properties due to their surface plasmon resonance effect which make them very useful in imaging and medical diagnostics [10–12], physical and chemical properties which enable them to be extremely beneficial in various fields including catalysts [13], biosensors [14], controlled drug delivery [15], and electronics [16]. It is important to state that these attractive features and properties are extremely dependent on their size, shape, coating materials, and aggregation status [17–19]. The preparation and application of gold nanoparticles (Au NPs) involve practical challenges that significantly impact their utility and efficacy. One key concern is the stability of Au NPs over time, a critical aspect for ensuring reproducibility and long-term functionality. Additionally, the removal of unreacted byproducts is a practical consideration that directly influences the purity and performance of the synthesized nanoparticles [20]. A wide variety of methodologies have been proposed for the synthesis of these nanoparticles such as chemical reduction using a reducing agent [21] seeded growth method [22], sonochemistry [23], laser pulse [24], and photochemistry [25]. However, all these approaches are expensive, hard to control, toxic and require a long treatment time as additional steps are needed in order to eliminate undesired chemicals from the solution [17]. Therefore, to overcome these issues, the development of an alternative synthesis methodology that is simple, rapid, and environmentally friendly without the use of harsh chemicals has become the direction of recent studies in order to obtain size controlled homogeneous gold nanoparticles [16, 17, 24, 26, 27]. Cold plasma in or in contact with the liquid is a one-phase, simple and cost-effective method for the synthesis of metal nanoparticles [28]. Due to the various reactive species, radicals (hydrogen, hydroxyl, and oxygen), electrons, and UV radiations present inside the plasma, this technique reduces metal ions dissolved in the liquid to neutral atoms at the gas-liquid interface [27, 29]. The biggest advantage about this process is that it offers an operating medium where it is possible to control the reactions inside the solutions in order to be able to tune the nanoparticles into the shape and size desired by modifying the chemical parameters [16]. In addition, the setup described herein could be used to prepare several metal nanoparticles directly into different matrix, e.g., solids as polymers or also hydrophilic and hydrophobic solvents, moreover, it could be easily scaled up for a pilot setup. In this present study, a helium atmospheric pressure plasma jet was used to synthesize spherical and mono-dispersed gold nanoparticles by only using gold (III) chloride hydrate ($HAuCl_4$) as a precursor and polyvinylpyrrolidone (PVP) as a capping agent/stabilizer. PVP has been reported to prevent the nanoparticles from growth and inhibit their agglomeration because of its hydrophobic carbon chains, which extend into solvents and interact with one another, providing repulsive forces [1, 30]. Acknowledging the intricate nature of Au NP synthesis, there is a multitude of factors that can influence the morphology of the obtained nanoparticles. While variations in plasma physical input parameters, such as input power supply current, frequency, and gas flow rate, can play a pivotal role in nanoparticle synthesis, it is imperative to note that these parameters remained constant throughout this study. Instead, the primary focus centered on the chemical parameters of the solution exposed to the plasma. The effects of PVP and $HAuCl_4$ concentrations on the size and the shape of the gold nanoparticles were investigated as well as the effect of the plasma exposure duration. This study will show that the synthesized gold nanoparticles could be effectively tuned in the nanometer range by adjusting the initial concentrations.

2. Experimental procedures

Gold (III) chloride hydrate ($HAuCl_4 \cdot xH_2O$, 99.995%, MW: 339.79 $g \cdot mol^{-1}$, Sigma-Aldrich) was dissolved in Ultrapure water (Direct-Q UV, Millipore) to get a 2 $mmol \cdot L^{-1}$ solution and stored as a stock solution. Polyvinylpyrrolidone (PVP, MW: 40 000 $g \cdot mol^{-1}$) was also purchased from Sigma-Aldrich and used as a capping agent for the nanoparticles. These two products were used as purchased with no further purification. The experimental device used to generate the plasma (figure S1 in the supplementary document) consists of a power supply purchased from OLISCIE company which uses a patented technology to apply fast voltage pulses on a capacitive load, a helium gas bottle connected to a gas flowmeter to regulate the gas intake and an asymmetric glass source. The plasma jet is initiated between the two elec-

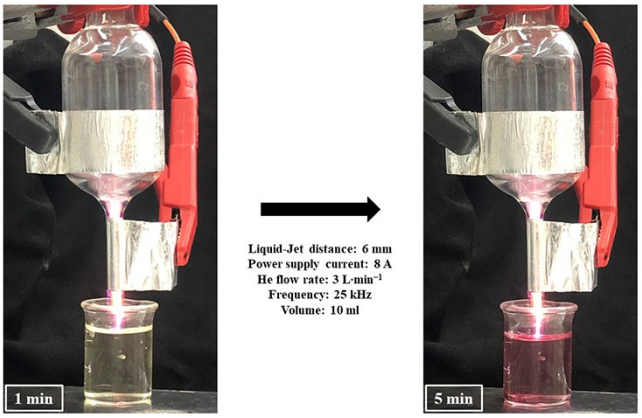

Figure 1. Pictures presenting the sample at (left) 1 min and (right) 5 min of plasma exposure.

trodes coiled around the source as shown in figure 1. A more detailed explanation of the experimental device and the optical emission spectrum of the plasma jet generated is found in a previous publication [31]. Using discharge plasma reduction, only one step was needed to synthesize gold nanoparticles from the $HAuCl_4$ and PVP aqueous solution. Different samples were prepared with $HAuCl_4$ concentration ranging from 0.1 to 2 mmol·L^{-1} and PVP concentration ranging from 0 to 0.1 mmol·L^{-1} in order to determine the optimal chemical conditions to obtain well separated and homogeneous nanoparticles. 10 mL of each resulting reaction medium was treated by the helium plasma jet for a certain amount of time at a power supply current of 8 A, a frequency of 25 kHz, 3 L·min^{-1} of gas flow rate and the distance between the end of the source and the liquid was fixed at 6 mm making sure that the plasma plume touches the surface of the liquid. The synthesized gold nanoparticles were characterized by UV-vis spectra in the 300–800 nm wavelength range using a UV-vis spectrophotometer (Evolution 60S) by Thermo Scientific to confirm the formation of gold nanoparticles by showing the plasmon resonance band. To measure the nanoparticles size distribution, the dynamic light scattering (DLS) analysis was used by Malvern Instruments Zetasizer (633 nm He–Ne laser). The solution was analyzed immediately after treatment to minimize the risk of agglomeration, as any post-treatment steps could potentially alter the nanoparticle characteristics. To determine the morphology of the synthesized nanoparticles, transmission electron microscopy (TEM) measurements were performed using the transmission electron microscope JEOL (JEM 100CX-II); the samples underwent a 10 min ultrasonic bath treatment to eliminate any possible agglomeration. After that, a drop of each sample was placed on a microscopy grid and dried at room temperature prior to the TEM measurements.

3. Results and discussion

3.1. Plasma setup characterization

Figure 2(a) shows the power supply discharge current in a time period. The peak measured was about 1.2 A. The species generated in the plasma jet were determined by optical emission spectrum in the previous publication [31] and the OES spectrum can be found in the supplementary document (figure S2). Three different species were chosen at different wavelengths to study their evolution over time. Figure 2(b) presents in the same graph, the power supply discharge current (red dashed line) with the emission lines of the helium (green line) at 587.5 nm, the N_2^+ (orange line) at 391.3 nm and the N_2 (blue line) at 337 nm. As can be seen from the graph, there is an overlap between the emission lines and the typical discharge current so this corroborated that the plasma discharge is responsible for the generation of the reactive species detected.

3.2. Effect of the plasma interaction duration on the Au NPs

To study the effect of the plasma interaction duration on the formation of the Au NPs, experiments were performed with 6 different discharge time durations ranging from 0 to 15 min (considering 0 as no plasma exposure) with $HAuCl_4$ and PVP concentrations of 1 mmol·L^{-1} and 0.05 mmol·L^{-1}, respectively. Figure 3 shows the UV-vis absorbance spectra of the treated solutions, the color change immediately after only 1 min of plasma exposure and the detectable absorbance band at around 530 nm appearing at 3 min are both an indicator of Au NPs formation. In figure 3(a), it can be seen that the intensity of the absorption band enhances with a longer plasma interaction which can be explained by an increase in the amount of the gold nanoparticles formed. At 15 min of interaction, the highest concentration of nanoparticles was obtained represented by the highest absorbance band as the spectrophotometer reached its saturation point and the deepest color between the samples (figure S3 in the supplementary document). To be able to study the morphology of the formed nanoparticles, figure 3(b) represents the normalized absorbance of the different samples. When the plasma exposure duration is increasing, a shoulder gradually starts to appear at a higher wavelength until a second broad band emerges, indicating that the size is increasing or two different sizes are present in the treated solution [32]. At 3 and 5 min of exposure, the plasmon bands are the most symmetric and very narrow with a full width at half maximum (FWHM) of 54 and 56 nm respectively which is a sign that the nanoparticles are mainly the same shape

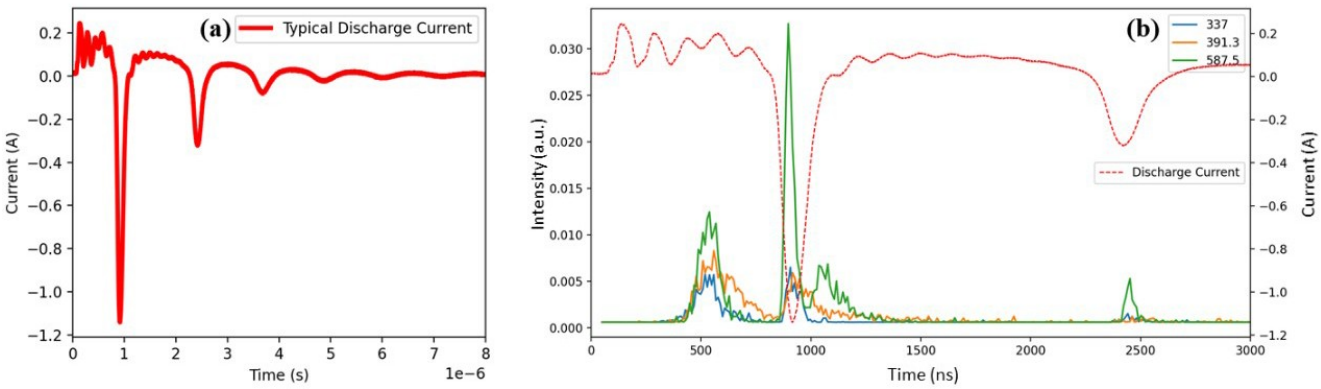

Figure 2. Graphs showing (a) the typical discharge current of the power supply as a function of the time and (b) the time evolution of He in green, N_2^+ in orange and N_2 in blue with the power supply discharge current.

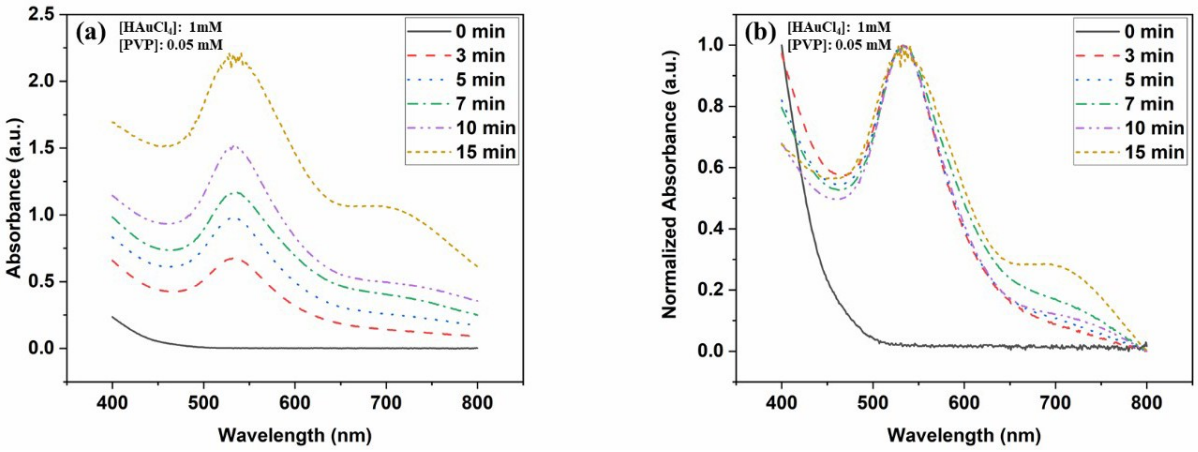

Figure 3. UV-vis (a) absorbance and (b) normalized absorbance spectra of the solutions with 1 mM of $HAuCl_4$ and 0.05 mM of PVP at different plasma exposure durations (from 0 to 15 min).

and size and the samples do not contain agglomerated particles [26]. So, for the further studies, 5 min was chosen as the plasma exposure duration because 3 min was not enough time for the synthesis rate to be efficient as the intensity of the absorbance band was very low compared to the other samples.

3.3. Effect of the precursor's concentration on the Au NPs

Several $HAuCl_4$ concentrations were studied to determine the influence of the precursor's concentration on the morphology and size distribution of the Au NPs. Shown in figure 4 is the UV-vis normalized absorbance spectra of 5 different solutions of $HAuCl_4$ concentrations ranging from 0.1 to 1.5 mmol·L^{-1} after 5 min of plasma discharge exposure at 0.05 mmol·L^{-1} of PVP. It is important to mention that understanding the LSPR peak position and shape helps to determine the average size and size distribution of the nanoparticles, providing crucial information about their morphology. Smaller nanoparticles typically exhibit an absorbance band at shorter wavelengths, while larger nanoparticles show bands at longer wavelengths. Additionally, the shape of the nanoparticles can lead to different spectral profiles. In our case, when the concentration is increased the position of the plasmon band is shifting to higher wavelength from 526 to 534 nm. This red shift is usually observed as the nanoparticle size increases [33]. Also, the uniformity of the Au NPs could be characterized by studying the FWHM of the absorption spectra [34]. The most symmetric and narrowest absorbance band at 526 nm and FWHM at 50 nm (figure S5 and table S3 in the supplementary document) were noted at the precursor's concentration of 0.1 mmol·L^{-1}.

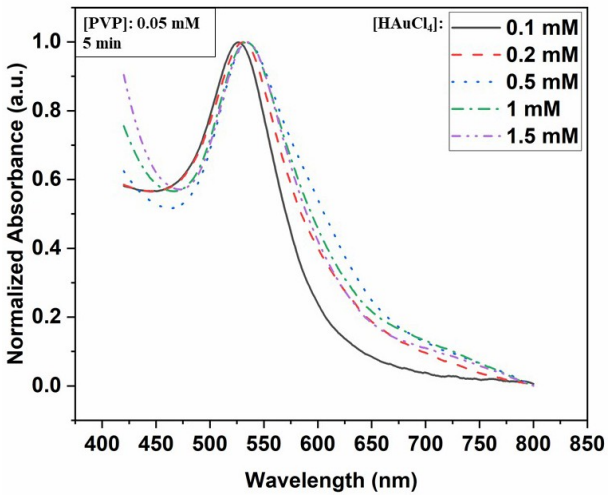

Figure 4. Normalized UV-vis absorbance spectra of the solutions after 5 min of plasma exposure with 0.05 mmol·L^{-1} of PVP at different $HAuCl_4$ concentrations.

Further investigation of the effect of $HAuCl_4$ has been conducted by transmission electron microscopy in order to examine the nanoparticle's morphology, as shown in figures 5 (a)–(e). The images reveal that the average size of the gold nanoparticles as well as their shape changes a lot with the increase of the precursor's concentration. In fact, in figure 5(a) at 0.1 mmol·L^{-1} of $HAuCl_4$, the nanoparticles were all spherical, very well-dispersed and homogeneous with an average diameter of 13±4 nm calculated by measuring 200 random nanoparticles in the TEM micrographs. While in figure 5(b) at 0.2 mmol·L^{-1}, the nanoparticles are larger with an average diameter of 27±7 nm (also by measuring 200 random nanoparticles) and some exotic shapes can be observed other than spheres such as triangles, rods, pentagons, etc. In figures 5(c)–(e) at 0.5, 1, and 1.5 mmol·L^{-1} respectively, it is obvious that the samples present a lot of aggregated nanoparticles. So, the optimal precursor's concentration to obtain spherical and uniform gold nanoparticles was 0.1 mmol·L^{-1}.

3.4. Effect of the PVP's concentration on the Au NPs

The impact of PVP concentrations on the size and shape of the gold nanoparticles was also examined because it is expected to have a significant effect [30], and this work aims to avoid the use of an excess chemical product. Under fixed plasma parameters and at 0.1 mmol·L^{-1} of $HAuCl_4$, different solutions were exposed to the plasma jet for 5 min with PVP

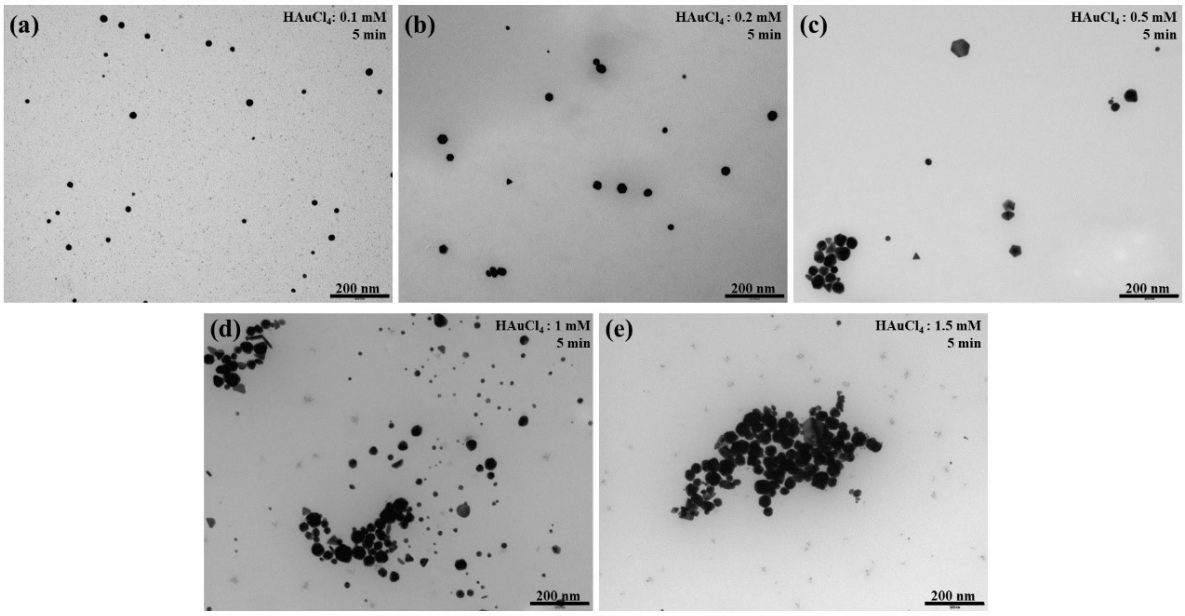

Figure 5. TEM micrographs of the sample solutions after 5 min of plasma exposure with 0.05 mmol·L^{-1} of PVP at (a) 0.1, (b) 0.2, (c) 0.5, (d) 1, and (e) 1.5 mmol·L^{-1} of $HAuCl_4$ concentrations.

concentration ranging from 0 to 0.1 mmol·L^{-1}. Figure 6 shows the normalized UV-vis spectra of the 7 different samples. The crucial role played by PVP became evident in the normalized UV-vis absorbance spectra, especially in the sample lacking the capping agent, which exhibited a noticeable distinct absorbance band at 550 nm signifying the presence of large particles. This optical behavior was confirmed by the TEM analysis in figure 7(a), where the nucleation and growing were carried out without control as shown in the image presenting large and aggregated gold particles. As PVP concentration was gradually increased, the λ_{max} shifted to lower wavelengths, this blue shift in the plasmon band is a consequence of a decrease in the size of the formed nanoparticles [35]. The microscopy images in figures 7(b)–(d) confirmed the formation of smaller sized gold nanoparticles

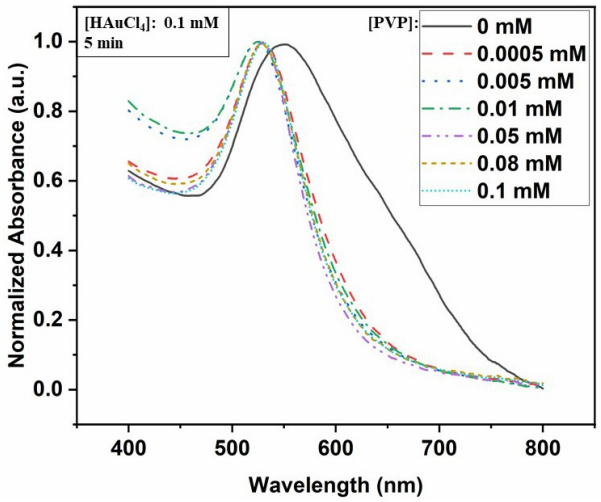

Figure 6. Normalized UV-vis absorbance spectra of the solutions after 5 min of plasma exposure with 0.1 mmol·L^{-1} of $HAuCl_4$ at different PVP concentrations.

and also showed some heterogeneous shapes as the samples present not only spherical forms but also some triangles, rods, hexagons, and of course some agglomerations were detected as well. Based on these analyses (one plasmon band and a FWHM of 47 nm in table S4 in the supplementary document) and the microscopy results in figure 7(e), the optimal PVP concentration was determined at 0.05 mmol·L^{-1}. In fact, this sample prepared with 0.1 mmol·L^{-1} of $HAuCl_4$ and 5 min of plasma exposure, the size of the particles obtained is consistent. From the TEM images, it was clear that all the nanoparticles have almost the same size with an average diameter of 13±4 nm obtained from measuring 200 randomly selected nanoparticles and the majority of them were spherical, very well-dispersed and separated. The samples obtained with a PVP concentration of 0.08 and 0.1 mmol·L^{-1}, as seen in figures 7(f)–(g), showed that the nanoparticles' shape changed with a larger variation in size and a tendency to agglomerate. It is observed that the agglomeration phenomena are multifaceted. In the case of PVP, its absence results in significant agglomeration due to the lack of a stabilizing agent, but as PVP is introduced, agglomeration diminishes, leading to the formation of well-separated nanoparticles, maintaining consistency in particle size at a 0.05 mM concentration. However, exceeding this threshold resulted in a different behavior, with small nanoparticles starting to agglomerate. This is consistent with findings by Guo *et al* [36], who reported that excess PVP can lead to nanoparticle aggregation until an equilibrium is reached. This suggests that the molar ratio of PVP to $HAuCl_4$ concentrations is the key factor to easily control the morphology of gold nanoparticles.

Finally, figure 8(a) presents the size distribution of gold nanoparticles prepared with the optimal parameters stated above obtained by DLS spectroscopy. The average size was 23±7 nm which matches with the size calculated by measur-

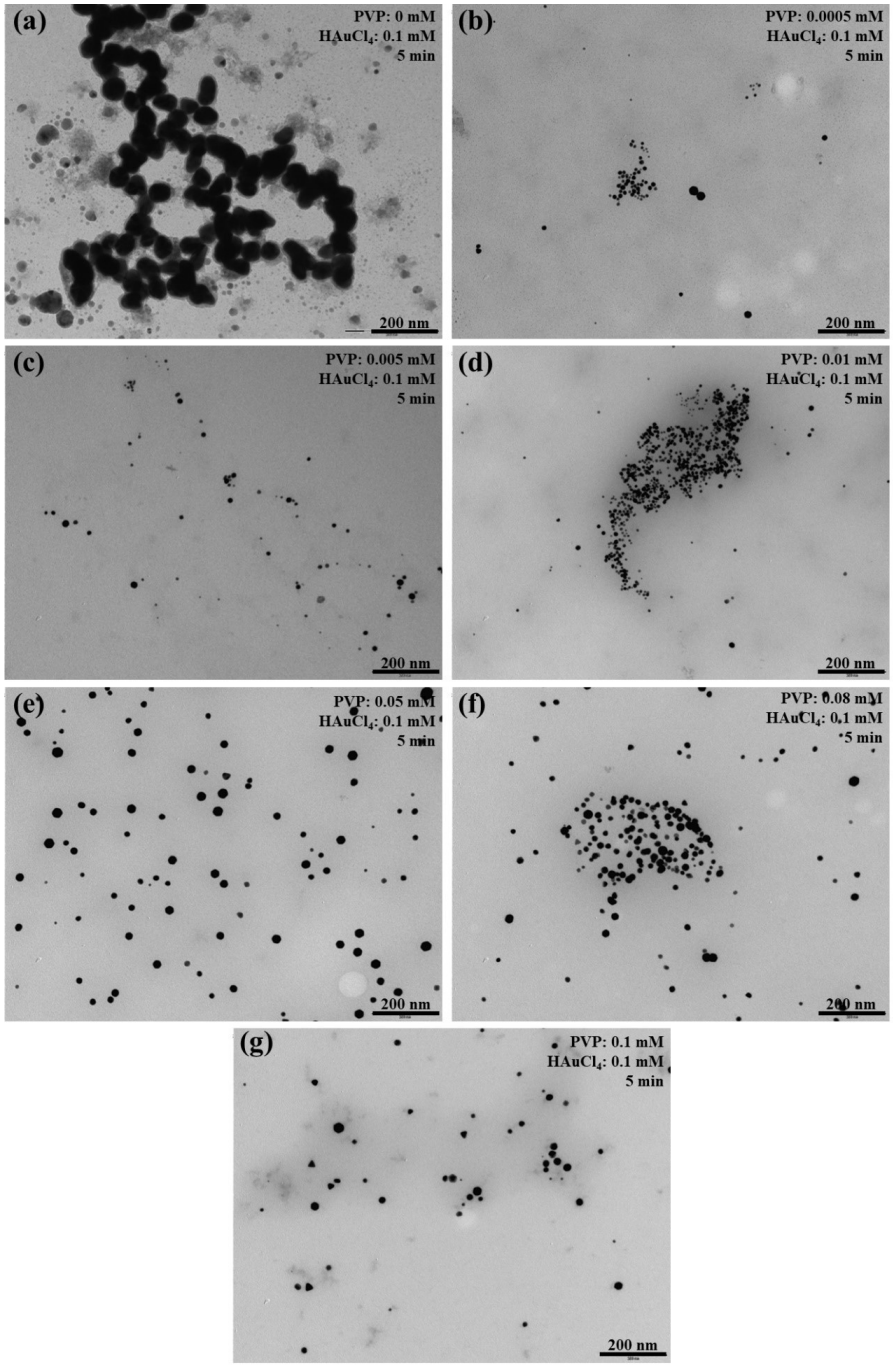

Figure 7. TEM micrographs of the solutions after 5 min of plasma exposure with 0.1 mmol·L^{-1} of $HAuCl_4$ at (a) 0 mmol·L^{-1}, (b) 0.0005 mmol·L^{-1}, (c) 0.005 mmol·L^{-1}, (d) 0.01 mmol·L^{-1}, (e) 0.05 mmol·L^{-1}, (f) 0.08 mmol·L^{-1}, and (g) 0.1 mmol·L^{-1} of PVP concentrations.

ing 200 random nanoparticles in the TEM images (13± 4 nm). The size obtained by DLS is slightly higher because it is the hydrodynamic size of the nanoparticles where the size obtained by TEM is the actual size of the solid nanoparticles.

XRD diffractogram as shown in figure 8(b) confirmed the formation of crystal structures of the synthesized gold nanoparticles after drying. The diffraction peaks obtained in the entire 2 theta region from 0° to 70° showed a cubic diffraction pattern (JCPD file No. 04-0784). The peaks at 38.24°, 44.45°, 64.67° correspond to the standard Bragg reflections (111), (200), and (220) of face center cubic lattice, respectively. In addition, the peak width is in agreement with the nanostructured sample.

A study amongst some of the articles synthesizing gold nanoparticles with different reduction techniques was conducted in order to compare these results with the literature and is summarized in table 1. The chemical reduction is known to be a very long process and additional steps are required in order to remove all the toxic chemicals and reducing agents from the final solution. The sonochemical and electrochemical techniques, despite their potential, often necessitate prolonged treatment periods and, in certain instances documented in the literature, fail to yield monodisperse nanoparticles. This plasma setup is the most efficient

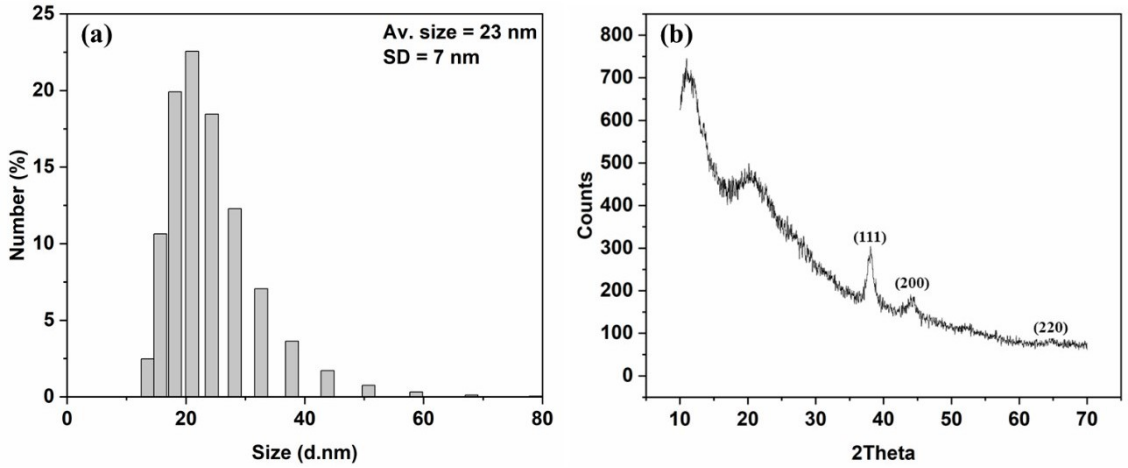

Figure 8. (a) Size distribution and (b) X-ray diffraction pattern of the synthesized Au NPs after 5 min of plasma exposure with 0.1 mmol·L^{-1} of $HAuCl_4$ and 0.05 mmol·L^{-1} of PVP.

Table 1. Different reduction methods for the synthesis of gold nanoparticles and the used chemical products, treatment time and the shape and size of the obtained Au Nps.

Reduction method	Precursor	Capping agent	Other products	Treatment time	Shape	Size (nm)	Reference
Chemical	$HAuCl_4 \cdot 3H_2O$	-	Sodium citrate (Reducing agent)	30 min	Spheres	12±2	[21]
Chemical	$HAuCl_4$	-	Chitosan (Reducing agent)	3 h	Spheres but not monodisperse	< 20	[37]
Chemical	$HAuCl_4$	Sodium citrate	$NaBH_4$ (reducing agent)	24 h	spheres	7±2	[38]
Sonochemical	$HAuCl_4$	PVP	1-propanol	120 min	Spheres, triangles, ellipse…	15–25	[39]
Sonochemical	$AuCl_4^-$	-	Ethanol	10 min	Spheres, triangle, rods…	23±7	[40]
Sonochemical	$HAuCl_4$	-	Silica spheres, ammoniac	45 min	Spheres	8	[41]
Electrochemical	$HAuCl_4$	PVP	KNO_3, SDBS	5–40 min	Spheres but not monodisperse	11.3±2.3	[42]
Electrochemical	$HAuCl_4 \cdot 4H_2O$	-	KCl	5 electrodeposition cylcles	Spheres	35±5	[43]
Plasma	$HAuCl_4$	Chitosan	-	15 min (3 h preparation time before)	Spheres	4	[44]
Plasma	$HAuCl_4 \cdot 4H_2O$	SDS	-	5 min 45 min	Triangles, pentagons, hexagons…	50 20	[19]
Plasma	$HAuCl_4 \cdot 3H_2O$	CTAB	NaOH	30 min	Spheres	2 (pH 12), 4 (pH 6), 10 (pH 3)	[16]
Plasma (present study)	$HAuCl_4 \cdot xH_2O$	PVP	-	5 min	Monodispersed spheres	13±4	-

in terms of treatment time as it takes only 5 min to elaborate the nanoparticles, the solution preparation time is also around 5 min, and the obtained nanoparticles are monodisperse, homogeneous with no agglomeration found in the samples. In addition, the proposed methodology can be scaled up and carried out in hydrophobic or hydrophilic mediums, gels, and also on solid substrates.

4. Conclusions

In this study, a non-thermal helium plasma jet proved to be a simple and cost-effective technique for the preparation of gold nanoparticles. Highly dispersed, homogeneous and uniform gold nanoparticles were successfully synthesized within only minutes of plasma discharge exposure. The effects of different synthesis parameters such as the plasma exposure duration, the precursor and stabilizer concentrations were studied in order to obtain the optimal results. This study showed that the size and shape of the gold nanoparticles could be easily tuned by adjusting the initial concentrations. As a result, to obtain the most uniform and spherical gold nanoparticles with an average diameter of 13 nm, the optimal conditions were found to be: 5 min of plasma treat-

ment duration, 0.1 mmol·L^{-1} $HAuCl_4$ concentration and 0.05 mmol·L^{-1} PVP concentration. Such gold nanoparticles may therefore be considered excellent candidates for various applications and can be used in many different fields. They can be used in biomedical applications as contrast agents for imaging, cancer treatments, drug delivery. They also possess distinct physical and chemical properties that make them excellent tools for the fabrication of novel chemical and biological sensors.

Acknowledgments

The authors acknowledge the Brazilian agencies FAPESP (Nos. 2018/10172-7 and 2019/18828-1) and CAPES (Finance Code 001), CNPq (No. 303580/2021-6), the National Institute of Photonics—INFO (INCTs program), the Universidade de São Paulo (USP), and Ministère de L' Enseignement Supérieur de la Recherche et de l'Innovation (France) for financial support.

References

[1] Hecold M *et al* 2017 *J. Nanomater.* **2017** 8706921
[2] Buraa M K, Obaid A S and Ali H H 2020 *IOP Conf. Ser.: Mater. Sci. Eng.* **928** 072059
[3] Bayda S *et al* 2020 *Molecules* **25** 112
[4] Etame A B *et al* 2011 *Nanomed.: Nanotechnol. Biol. Med.* **7** 992
[5] Das M *et al* 2011 *Toxicol. Environ. Health Sci.* **3** 193
[6] Buzea C, Pacheco I I and Robbie K 2007 *Biointerphases* **2** MR17
[7] Wang Y Q, Liang W S and Geng C Y 2009 *Nanoscale Res. Lett.* **4** 684
[8] Bell A T 2003 *Science* **299** 1688
[9] Kundu S, Wang K and Liang H 2009 *J. Phys. Chem. C* **113** 134
[10] Shin H S *et al* 2004 *J. Colloid Interface Sci.* **274** 89
[11] Wang H S *et al* 2005 *Coll. Surf. A: Physicochem. Eng. Aspects* **256** 111
[12] Zarschler K *et al* 2016 *Nanomed.: Nanotechnol. Biol. Med.* **12** 1663
[13] Boyen H G *et al* 2002 *Science* **297** 1533
[14] He L *et al* 2000 *J. Am. Chem. Soc.* **122** 9071
[15] Siddique S and Chow J C L 2020 *Appl. Sci.* **10** 3824
[16] Bratescu M A *et al* 2011 *J. Phys. Chem. C* **115** 24569
[17] Chen Q, Kaneko T and Hatakeyama R 2012 *Chem. Phys. Lett.* **521** 113
[18] Furusho H *et al* 2009 *Chem. Mater.* **21** 3526
[19] Hieda J, Saito N and Takai O 2008 *J. Vac. Sci. Technol. A* **26** 854
[20] Balasubramanian S K *et al* 2010 *Biomaterials* **31** 9023
[21] Jana N R, Gearheart L, Murphy C J 2001 *Chem. Mater.* **13** 2313
[22] Pérez-Juste J *et al* 2005 *Coord. Chem. Rev.* **249** 1870
[23] Oshima R *et al* 1999 *Nanostruct. Mater.* **12** 111
[24] Liang X, Wang Z J and Liu C J 2010 *Nanoscale Res. Lett.* **5** 124
[25] Dong S A and Zhou S P 2007 *Mater. Sci. Eng.: B* **140** 153
[26] Xuan L T Q, Nguyen L N and Dao N T 2022 *Nanotechnology* **33** 105603
[27] Saito N, Hieda J and Takai O 2009 *Thin Solid Films* **518** 912
[28] Gonçalves J M *et al* 2019 *J. Mater. Sci.: Mater. Electron.* **30** 16724
[29] Takai O 2008 *Pure Appl. Chem.* **80** 2003
[30] Koczkur K M *et al* 2015 *Dalton Trans.* **44** 17883
[31] Habib T *et al* 2022 *Nanotechnology* **33** 325603
[32] Kim S M, Kim G S and Lee S Y 2008 *Mater. Lett.* **62** 4354
[33] Pimpang P and Choopun S 2011 *Chiang Mai J. Sci.* **38** 31
[34] Amendola V and Meneghetti M 2009 *J. Phys. Chem. C* **113** 4277
[35] Kreibig U and Genzel L 1985 *Surf. Sci.* **156** 678
[36] Guo S and Wang E 2007 *Inorg. Chem.* **46** 6740
[37] Wei D W and Qian W P 2008 *Colloids Surf. B: Biointerfaces* **62** 136
[38] Chaudhary A and Garg S 2017 *Mater. Sci. Eng.: C* **80** 18
[39] Okitsu K, Ashokkumar M and Grieser F 2005 *J. Phys. Chem. B* **109** 20673
[40] Caruso R A, Ashokkumar M and Grieser F 2002 *Langmuir* **18** 7831
[41] Pol V G, Gedanken A and Calderon-Moreno J 2003 *Chem. Mater.* **15** 1111
[42] Ma H Y *et al* 2004 *Chem. Phys. Chem.* **5** 68
[43] Hu Y L *et al* 2011 *Thin Solid Films* **519** 6605
[44] Jin Y *et al* 2013 *Carbohyd. Polym.* **91** 152